

## Research Article

# Modified Yuejuwan Inhibited Cholesterol Accumulation and Inflammation in THP-1 Macrophage-Derived Foam Cells by Inhibiting the Activity of the TRIM37/TRAF2/NF- $\kappa$ B Pathway

Mingtai Gui, Lei Yao, Bo Lu, Jianhua Li, Jing Wang, Xunjie Zhou, and Deyu Fu 

Department of Cardiology, Yueyang Hospital of Integrated Traditional Chinese and Western Medicine, Shanghai University of Traditional Chinese Medicine, Shanghai, China

Correspondence should be addressed to Deyu Fu; [fdy65sci2019@126.com](mailto:fdy65sci2019@126.com)

Received 17 September 2021; Accepted 25 January 2022; Published 10 March 2022

Academic Editor: Wen yi Kang

Copyright © 2022 Mingtai Gui et al. This is an open access article distributed under the Creative Commons Attribution License, which permits unrestricted use, distribution, and reproduction in any medium, provided the original work is properly cited.

**Background.** This study aimed to explore the function of modified Yuejuwan (MYJ) on THP-1 macrophage-derived foam cells. **Methods.** First, human THP-cells were obtained, and then, grouping was made to the following: control group, foaming group, foaming group +0.2 mg/mL Jiawei Yueju pill, foaming group +0.5 mg/mL Jiawei Yueju pill, and foaming group +1 mg/mL Jiawei Yueju pill. An Oil Red O staining assay was used to examine the uptake of oxidatively modified low-density lipoprotein (oxLDL). The secretion of interleukin (IL)-1 $\beta$  and tumor necrosis factor (TNF)- $\alpha$  were determined using an enzyme-linked immunosorbent assay (ELISA). Real-time quantitative PCR (qRT-PCR) and Western blot were used to quantify genes and proteins expression levels. **Results.** Our results indicated that MYJ inhibited the accumulation of total cholesterol (TC), free cholesterol (FC), and cholesteryl ester (CE) in foam cells. Moreover, the secretion of IL-1 $\beta$  and TNF- $\alpha$  also downregulated in foam cells after treatment of MYJ. Furthermore, we found that tripartite motif-containing 37 (TRIM37) was significantly upregulated in foam cells. Knockdown of TRIM37 promoted cholesterol efflux and presented an anti-inflammation effect in foam cells. Furthermore, TRIM37 positively mediated the translocation of NF- $\kappa$ B to nuclear. It negatively regulated its ubiquitination in foam cells after interacting with TRAF2. Importantly, MYJ profoundly suppressed the function of TRIM37 in foam cells and functioned as a TRIM37 inhibitor. **Conclusions.** This study demonstrated that MYJ might alleviate oxLDL-induced foam cell formation by inhibiting the TRIM37/TRAF2/NF- $\kappa$ B pathway activity. MYJ was a potential agent in preventing atherosclerosis and indicated its potential signaling pathway in foam cells.

## 1. Background

Atherosclerosis is a chronic inflammatory disease of the arterial wall, which is the most common underlying pathology of cardiovascular diseases (CVDs). CVDs are the most common cause of death worldwide, killing 17.5 million people, representing more than 30% of all global deaths [1, 2]. It is characterized by complex atherosclerotic plaques [3]. The process is deeply influenced by endothelial abnormal vascular inflammation, the proliferation of vascular smooth muscle cells, thrombus formation, and conversion of macrophages into foam cells [4]. Moreover, foam cells had been confirmed as the major culprit in atherosclerosis [5]. Targeting the formation of

foam cells provides novel insight for fighting atherosclerosis and CVD [6].

Tripartite motif-containing 37 (TRIM37), containing RING finger region, is located in the 17q23 chromosomal region [7]. As an E3 ubiquitin ligase, TRIM37 is instrumental in regulating the inflammatory cascade [8]. Moreover, TRIM37 has a TNF-receptor associated factor (TRAF) sequence and enhances K63-linked ubiquitination of TRAF2 [9]. Furthermore, a previous report demonstrated that TRIM21 influences atherosclerosis through regulating Th17 [10]. Nuclear factor- $\kappa$ B (NF- $\kappa$ B), a downstream factor of TRAF2, is reported as a proatherogenic factor [11], and activated NF- $\kappa$ B is closely associated with foam cell formation and vascular inflammation [12, 13]. Moreover, it

confirmed that NF- $\kappa$ B inhibitors suppress the formation of foam cells and atherosclerotic plaque accumulation [14]. Therefore, inhibiting NF- $\kappa$ B activity provided novel insight into the treatment for atherosclerosis.

Yuejuwan (YJ), a traditional Chinese medicine (TCM), is widely used for digestive dysfunction and depressive illness [15]. The newer version of the YJ, now being called modified Yuejuwan (MYJ), contributes to the formation of hepatic macrovesicular steatosis and reduces inflammatory infiltration in a nonalcoholic fatty liver disease rat model [16]. MYJ presented a clinical curative effect on removing dampness to reduce phlegm, invigorating the blood circulation, and eliminating stasis [17, 18]. However, the underlying effect of MYJ on foam cells is still unclear.

The target of the present study is to explore the effect of MYJ on human foam cells. Moreover, we also examined the role of TRIM37 in foam cells in the presence of MYJ. Our finding not only gained a deep insight into the biological effect of MYJ but also indicated its potential molecule pathway in human foam cells.

## 2. Methods

**2.1. Study Design.** A total of 207 g Jiawei Yueju was purchased and put in a special decoction pot, decocted on high heat until the water was boiled, fried slowly on low heat for about 45 minutes, and filter out 500 ml of liquid medicine. The medicinal solution was divided into a  $-80^{\circ}\text{C}$  refrigerator and stored overnight and then put into a freeze-dried agent for freeze-drying. After 72 h, a powdered drug freeze-dried powder was obtained. Then, grouping was made as follows: control group, foaming group, foaming group +0.2 mg/mL Jiawei Yueju pill, foaming group +0.5 mg/mL Jiawei Yueju pill, and foaming group +1 mg/mL Jiawei Yueju pill. The basis for concentration selection is unknown.

**2.2. Cell Culture.** Human THP-1 cells were obtained from the cell bank of Shanghai Biology Institute (Shanghai, China). Cells were seeded in DMEM medium (Trueline, USA) containing FBS (10%, 16000-044, Gibco, USA) and penicillin-streptomycin solution (1%, P1400-100, Solarbio, China). All cells were incubated with the condition of 5%  $\text{CO}_2$  at  $37^{\circ}\text{C}$ . Then, THP-1 cells were primed with phorbol-12-myristate-13-acetate (PMA, 100 nM; P1585, Sigma, USA) for 24 h at  $37^{\circ}\text{C}$  to differentiate into macrophages and followed incubation with oxidatively modified low-density lipoprotein (oxLDL, 50 mg/L; H7950, Solarbio, China) for 48 h to transform these macrophages into foam cells [19–21].

**2.3. Oil Red O Staining.** Foam cells were fixed with paraformaldehyde solution for 30 min at room temperature after being washed twice with phosphate buffer solution (PBS). After that, cells were stained with Oil Red O for half an hour. The image of stained cells was collected using microscopy (XDS-600C, Caikon, Shanghai, China) on 200X.

**2.4. RNA Extraction and Real-Time Quantitative PCR (qRT-PCR) Analysis.** Total RNA was extracted using the TRIzol reagent kit (1596-026, Invitrogen, USA) and then converted into cDNA according to the instruction of the manufacture (#K1622, Fermentas, Canada). The experiment was established on real-time detection (ABI-7300, ABI, USA) using SYBR Green master mix (#K0223, Thermo, USA). Relative gene expression determination was counted according to the  $2^{-\Delta\Delta\text{Ct}}$  method using  $\beta$ -actin as an endogenous reference. The primer sequences used in this study are given in Table 1.

**2.5. Overexpression and Knockdown of TRIM37 in Foam Cells.** For overexpression of TRIM37, the entire length of TRIM37 cDNA was inserted into the lentiviral vector (pLVX-Puro; Catalog No. 632164; Clontech Laboratories Inc., USA). Then, the recombinant vector (pLVX-Puro-oeTRIM37) was transfected into foam cells. Meanwhile, the mock vector functioned as the corresponding negative control (oeNC), and three short interfering RNAs (siRNA) that target different regions of human gene TRIM37 (NM\_001005207.4) were synthesized and subsequently transfected into foam cells (siTRIM37-1, siTRIM37-2, and siTRIM37-3). A non-specific scramble siRNA acted as the negative control (siNC). TRIM11siRNAs were provided as follows: siTRIM37-1 (1799–1817): GGAGAAGATTCAGAATGAA; siTRIM37-2 (2119–2137): CCAGTAGTTTACTAGACAT; siTRIM37-3 (2730–2748): GCCTTGATACATGGCAGTA.

**2.6. Western Blotting.** Total protein was isolated using RIPA lysis buffer (JRDUN, Shanghai, China). 25  $\mu\text{g}$  protein of each sample was fractionated and transferred onto PVDF nitrocellulose membrane (HATF00010, Millipore, USA) for 12 h. The transfer method was semidry at 25 V on 100 mA current, lasted for 30 minutes, and the pore size of the PVDF membrane was 0.22  $\mu\text{m}$ . Then, the membranes were probed with the primary antibodies overnight at  $4^{\circ}\text{C}$ , followed by the appropriate HRP-conjugated goat anti-rabbit IgG (A0208, Beyotime, China). Protein signals were analyzed using a chemiluminescence system. The antibodies details were provided as follows: TRIM37 (Ab95997, Abcam, UK, 1:1000), TRAF2 (Ab60169, Abcam, UK, 1:1500), SR-B1 (Ab52629, Abcam, UK, 1:1000), ABCA1 (Ab18180, Abcam, UK, 1:1000), ABCG1 (Ab52617, Abcam, UK, 1:2000), NF-KB (#8242, CST, USA, 1:1000), H3 (#4499, CST, USA, 1:1000), and  $\beta$ -actin (#4970, CST, USA, 1:1000).

**2.7. Enzyme-Linked Immunosorbent Assay (ELISA).** According to the manufacture protocol, initially, the protein cells were extracted from the incubator, and the culture solution was aspirated. Then, washed twice with precooled  $1 \times$  PBS, aspirated the PBS, added a lysis buffer containing protease and phosphatase inhibitors, and fully lysed at  $4^{\circ}\text{C}$ . The cells were then scraped into a 1.5 ml EP tube, heated at  $95^{\circ}\text{C}$  for 10 minutes, and centrifuged at 12000 g for 10 minutes. The supernatant was taken, and the protein was quantified and stored in a refrigerator at  $-80^{\circ}\text{C}$  for WB detection. The secretion of IL-1 $\beta$  and TNF- $\alpha$  in foam cells

TABLE 1: Sequences for the primers used in the research.

Name	Primer sequences (5'-3')
TRIM8F	5'-CAGCCGTCCACCAAACACTAC-3', R 5'-ACCTCTGCGTCCAGGAGATTC-3'
TRIM13F	5'-TGCCCAGTAGCCTCTAGTTC-3', R 5'-GGCCAGGTGCTGTTATTCTC-3'
TRIM14F	5'-GGATTTGTGTCTCCGTTCTG-3', R 5'-TCTGTCTGCCTGGTATTCTG-3'
TRIM22F	5'-TCCATAGCAAAGCATCATAG-3', R 5'-GACAATGTGAAGAGTCATAG-3'
TRIM37F	5'-TGGACTTACTCGCAAATG-3', R 5'-ATCTGGTGGTGACAAATC-3'
TRIM39F	5'-GATCACTCGCTGCAAGTCC-3', R 5'-CACCTGCTGCTCTTCATCC-3'
ACTBF	5'-GATGACCCAGATCATGTTTGGAG-3', R 5'-TAATGTCACGCACGATTTC-3'

was determined by ELISA kits (IL-1 $\beta$ : GS-E10083, X-Y Biotechnology, China; TNF- $\alpha$ : XY-E10110, X-Y Biotechnology, China).

**2.8. Measurement of Lipid Levels.** The free cholesterol (FC) content detection kit (cat#BC1895; specification: 100 T/96 S; Solarbio, China) and total cholesterol (T-CHO) test kit (cat#A111-1; COD-PAP method single reagent; Njcbio, China) were purchased. According to the manufacture protocol, the levels of total cholesterol (TC) and FC were quantified. The difference value between TC and FC was counted as the content of cholesteryl ester (CE).

**2.9. Coimmunoprecipitation (Co-IP).** In brief, cell lysates were isolated after transfection or stimulation with appropriate ligands. Then, all samples were incubated by TRIM37, TRAF2, SR-B1, ABCA1, ABCG1, NF-KB, H3, and  $\beta$ -actin antibodies plus protein A/G beads (SantaCruz Biotechnology, USA) overnight before they were separated by SDS-PAGE.

**2.10. Ubiquitination Assay.** Foam cells transfected with siNC or siTRIM37 were lysed by sonication in 1% SDS-containing radioimmunoprecipitation assay (RIPA) buffer on ice. Then, lysates were treated by protein A/G plus agarose (sc-2003, Santa Cruz Biotechnology, USA) for 1 h. After that, each sample was incubated with IgG (sc-2027, Santa Cruz Biotechnology, USA) overnight at 4°C. Then, the nuclear pellet was gathered by centrifugation at 3000 rpm for 5 min at 4°C and subsequently washed by protein A/G Plus-Agarose beads four times. The purified proteins were run on 4–20% gradient SDS-PAGE. Anti-TRAF2 antibody (Ab60169, Abcam, UK) and antiubiquitin antibody (ab7780, Abcam, UK) were used for immunoblotting.

**2.11. Data and Statistical Analysis.** All values are expressed as means  $\pm$  S.E.M and analyzed with GraphPad Prism software V7.0 (California, USA). The results were assessed by analysis of variance (ANOVA) with LSD. Each analysis was performed in triplicate for all the procedures. *P* values <0.05 were considered statistically significant.

### 3. Results

**3.1. OxLDL Induced the Formation of Human THP-1 Macrophage Foam Cells.** Oil Red O staining assay was used to

determine oxLDL uptake in foam cells and revealed that oxLDL uptake was much higher in foam cells than in THP-1 cells (Figure 1(a)). In addition, TC, FC, and CE were quantified and found that accumulation of TC, FC, and CE significantly upregulated in foam cells than that of THP-1 cells (Figure 1(b)). The relative mRNA levels of TRIM8, TRIM14, and TRIM37 were upregulated in foam cells, especially for TRIM37 (Figure 1(c)). The translocation of NF- $\kappa$ B to nuclear also increased in foam cells (Figure 1(d)).

**3.2. MYJ Inhibited the Accumulation of Cholesterol in THP-1 Macrophage-Derived Foam Cells.** Foam cells were cultured with MYJ at different concentrations, including 0, 0.2, 0.5, and 1 mg/mL, to assess the function of MYJ on foam cells. As shown in Figure 2(a), the MYJ treatment suppressed the uptake of oxLDL in foam cells as the concentration rising. Moreover, the production of TC, FC, and CE downregulated in foam cells in the presence of MYJ (Figure 2(b)). Besides, IL-1 $\beta$  and TNF- $\alpha$  are important proinflammatory cytokines [22]. In this analysis, MYJ treatment decreased the expression of IL-1 $\beta$  and TNF- $\alpha$  in foam cells (Figure 2(c)).

Moreover, scavenger receptor-B1 (SR-B1), ATP-binding cassette transporter A1 (ABCA1), and ATP-binding cassette transporter G1 (ABCG1) prevent the accumulation of cholesterol in cells by promoting cholesterol efflux to lipid-poor apolipoprotein A-I [23]. Our results suggested that the protein contents of SR-B1, ABCA1, and ABCG1 profoundly decreased in foam cells than in THP-1 cells, whereas significantly recovered by MYJ treatment in a dose-dependent manner (Figure 2(d)). Taken together, these results suggested that MYJ might contribute to cholesterol efflux by positively regulating ABCA1, ABCG1, and SR-B1 in foam cells.

**3.3. Overexpression and Knockdown of TRIM37 in Foam Cells.** To address TRIM37 function in foam cells, TRIM37 induced overexpression and knockdown in foam cells. The relative mRNA and protein levels of TRIM37 remarkably increased in oeTRIM37 transfected cells. As shown in Figure 3(a), all TRIM37 siRNAs significantly disrupted the endogenous expression of TRIM37 in foam cells, especially for siTRIM37-1 and siTRIM37-2, which to be further investigated in a future study with extended experimental plans.

**3.4. TRIM37 Silencing Promoted Cholesterol Efflux in Foam Cells.** Then, we examined the uptake of oxLDL in siTRIM37

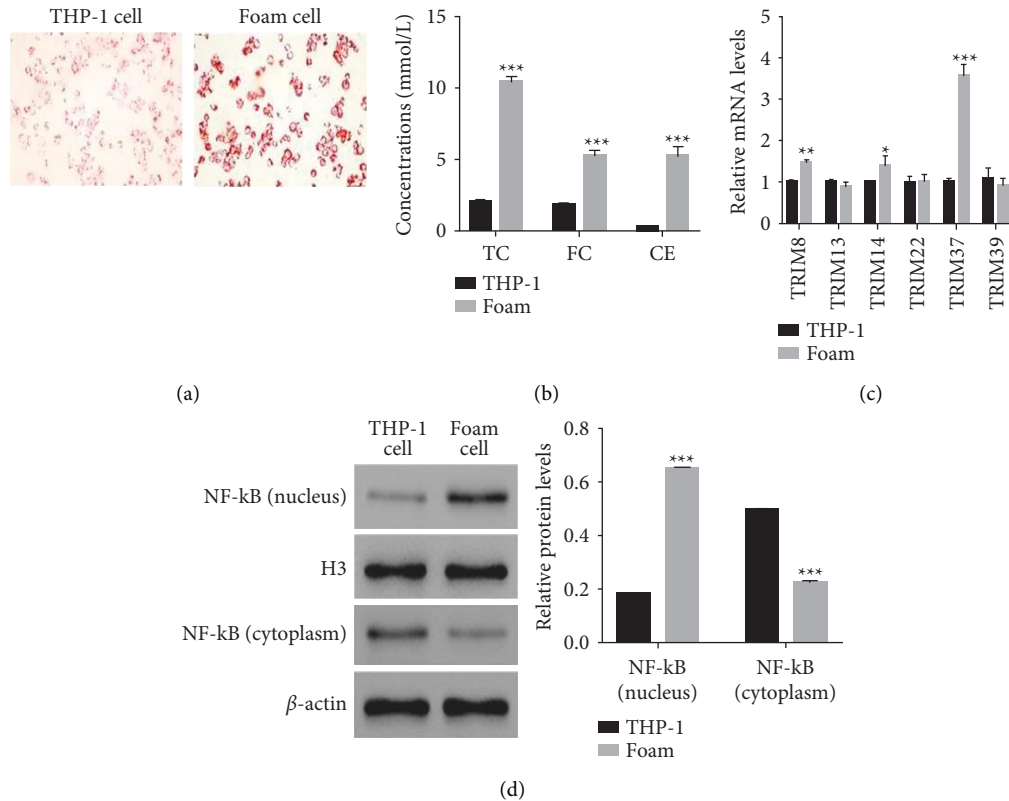


FIGURE 1: OxLDL induced the formation of human THP-1 macrophage foam cells. (a) Oil Red O staining indicating that oxLDL uptake upregulated in foam cells. Magnification: 200x. (b). The contents of TC, FC, and CE increased in foam cells. \*\*\*  $P < 0.001$  vs. THP-1. (c) qRT-PCR used to examine the relative mRNA levels of TRIM8, TRIM13, TRIM14, TRIM22, TRIM37, and TRIM39 in THP-1 and foam cells, respectively. \*  $P < 0.05$  vs. THP-1, \*\*  $p < 0.01$  vs. THP-1, \*\*\*  $p < 0.001$  vs. THP-1. (d) The translocation of NF- $\kappa$ B promoted in foam cells. \*\*\*  $P < 0.001$  vs. THP-1.

transfected cells. The accumulation of oxLDL in siTRIM37 transfected cells decreased greatly. Both siTRIM37-1 and siTRIM37-2 have deeply suppressed the production of TC, FC, and CE in foam cells (Figure 3(b)). Importantly, our results revealed that the expression of IL-1 $\beta$  and TNF- $\alpha$  deeply decreased in siTRIM37-1 or siTRIM37-2 transfected cells (Figure 3(c)). More importantly, TRIM37 silencing significantly suppressed the translation of SR-B1, ABCA1, and ABCG1 in foam cells. These findings suggested that siTRIM37 might promote cholesterol efflux by inhibiting ABCA1, ABCG1, and SR-B1 in foam cells (Figure 3(d)).

**3.5. TRIM37 Interacted with TRAF2 and Negatively Mediated Its Ubiquitination in Foam Cells.** Next, we examined the protein content of TRAF2 in siTRIM37-1 or siTRIM37-2 transfected cells. As shown in Figure 4(a), the protein content of TRAF2 significantly downregulated in siTRIM37-1 or siTRIM37-2 transfected cells. Moreover, results from the Co-IP assay indicated that TRIM37 interacted with TRAF2 in foam cells (Figure 4(b)). Notably, the knockdown of TRIM37 enhanced the ubiquitination of TRAF2 in foam cells (Figure 4(c)). Therefore, TRIM37 silencing might suppress the translocation of TRAF2 via enhancing its ubiquitination in foam cells.

**3.6. MYJ Inhibited the Function of TRIM37 in Foam Cells.** To further address the relationship between TRIM37 and MYJ, the oeTRIM37 transfected cells were cultured in the presence of MYJ (0.5 mg/mL). TRIM37 overexpression promoted the uptake of oxLDL in foam cells, but this function was suppressed with the treatment of MYJ (Figure 5(a)). Moreover, the contents of TC, FC, and CE were also deeply suppressed by MYJ in oeTRIM37 transfected cells (Figure 5(b)). Furthermore, our results revealed that TRIM37 overexpression promoted the expression of IL-1 $\beta$  and TNF- $\alpha$  in foam cells. However, this effect was also disrupted with the treatment of MYJ (Figure 5(c)). Meanwhile, TRIM37 overexpression promoted the translocation of NF- $\kappa$ B to nuclear in foam cells (Figure 5(d)). Taken together, these results demonstrated that MYJ presented the effects as a TRIM37 inhibitor in foam cells.

## 4. Discussion

Modified Yuejuwan (MYJ), a traditional Chinese medicine (TCM) widely used for mood disorders, has shown a curative effect on reducing phlegm, stimulating blood circulation, and eliminating stasis [15, 17, 18]. The underlying effect of MYJ in atherosclerosis remains unknown. This study explored the biological effect of MYJ and revealed its potential molecular pathway in human foam cells. After

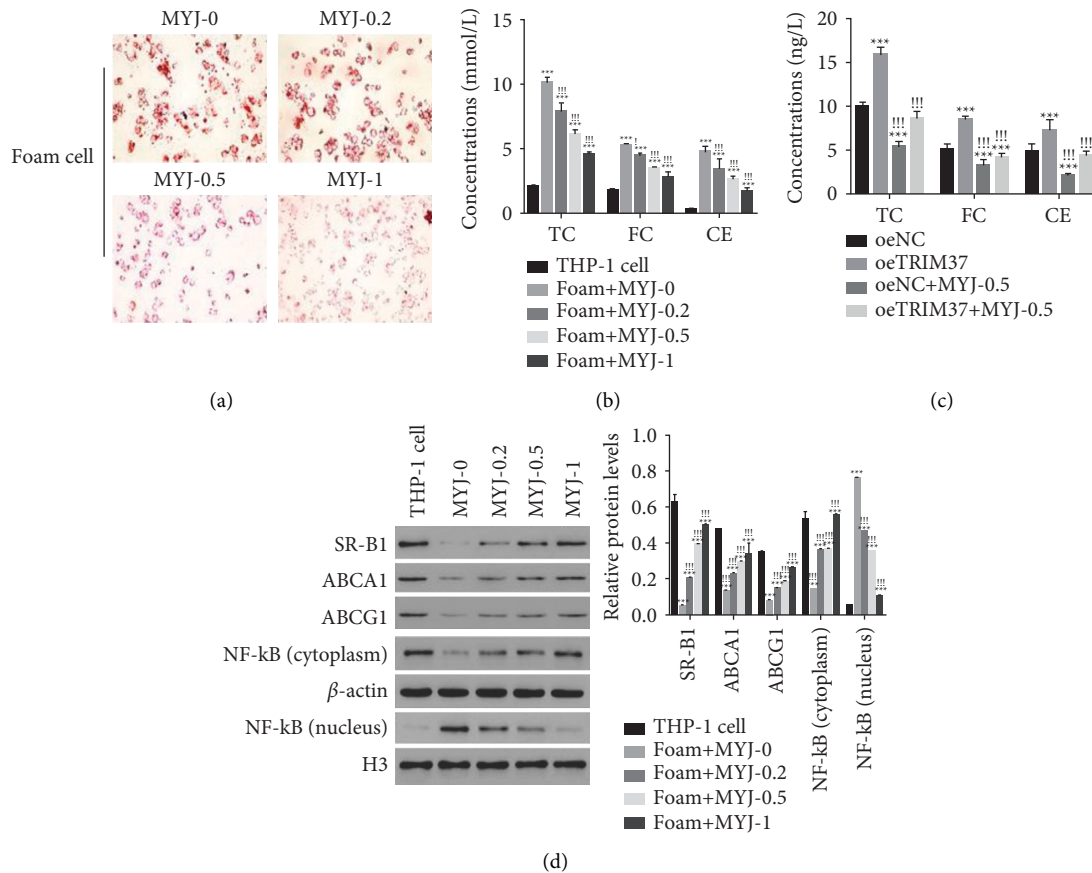


FIGURE 2: MYJ increased cholesterol efflux in THP-1 macrophage-derived foam cells. (a) MYJ treatment reducing oxLDL uptake in foam cells. Magnification: 200x. (b) MYJ treatment inhibiting the accumulation of TC, FC, and CE in foam cells. \*\*\*  $P < 0.001$  vs. THP-1,  $^{\dagger} p < 0.05$  vs. foam + MYJ-0,  $^{\#\#\#} p < 0.001$  vs. foam + MYJ-0. (c) The contents of IL-1 $\beta$  and TNF- $\alpha$  decreased in foam cells in the presence of MYJ. \*\*\*  $P < 0.001$  vs. THP-1;  $^{\#\#} p < 0.01$  vs. foam + MYJ-0,  $^{\#\#\#} p < 0.001$  vs. foam + MYJ-0. (d) Western blot used to examine the protein contents of SR-B1, ABCA1, ABCG1, NF- $\kappa$ B (cytoplasm), and NF- $\kappa$ B (nucleus) in cells as indicated above. \*\*\*  $P < 0.001$  vs. THP-1;  $^{\#\#\#} p < 0.001$  vs. foam + MYJ-0.

treating with MYJ, the secretion of IL-1 $\beta$  and TNF- $\alpha$  was downregulated, whereas TRIM37 was upregulated in foam cells. MYJ is effective for relieving depression, regulating digestion, and improving the emotional state [24]. So far, MYJ was found to be effective in the glutamate-induced HT22 cell injury model and used in different diseases [25, 26].

Foam cells and macrophages with engorging cholesterol are the major causes of atherosclerosis [27]. Therefore, inhibiting the transform of macrophages into foam cells draws much attention in the treatment of atherosclerosis. Fullerene derivatives, vitamin E, and apolipoprotein A-I mimetic peptide D4F can ameliorate the formation of oxLDL-induced foam cells [14, 28, 29]. In this study, we investigated the function of MYJ in THP-1 macrophage-derived foam cells. The findings of this study elucidated the potential value of MYJ in the prevention of atherosclerosis.

TRIM37 is known for its RING domain, B-box motifs, a coiled-coil region, and a C-terminal part that includes the MATH domain. TRIM37 deficiency is plagued with numerous tumors. A wide variety of cancers are associated with overexpression of TRIM37 [30]. TRIM37 is also an essential

determinant of mitotic vulnerability to PLK4 inhibition [31]. Nonetheless, TRIM37 participates in K63 polyubiquitination of TRAF2, which is a significant step in the activation of NF- $\kappa$ B signaling [9].

NF- $\kappa$ B activation is widely recognized as a pathological mechanism of the lipid metabolism and atherosclerosis [32]. On the other hand, TRAF2 is reported as an adaptor factor and mediates NF- $\kappa$ B activation [33]. Moreover, TRIM37 ubiquitylates PEX5 at K464 to promote peroxisomal matrix protein import [34]. In this analysis, our results indicated that MYJ inhibited the translocation of NF- $\kappa$ B to nuclear and suppressed the translation of TRAF2 in foam cells. In addition, TRIM37 was identified as upregulation in THP-1 macrophage-derived foam cells. Moreover, TRIM37 interacted with TRAF2 and negatively mediated its ubiquitination in foam cells. TRIM37 possibly serves different functions in regulating TRAF2 ubiquitination in different cells.

Importantly, we found that MYJ functioned as a TRIM37 suppressor in foam cells. Taken together, all these findings indicated that MYJ might alleviate oxLDL-induced foam cell formation by inhibiting the activity of the TRIM37/TRAF2//NF- $\kappa$ B pathway.

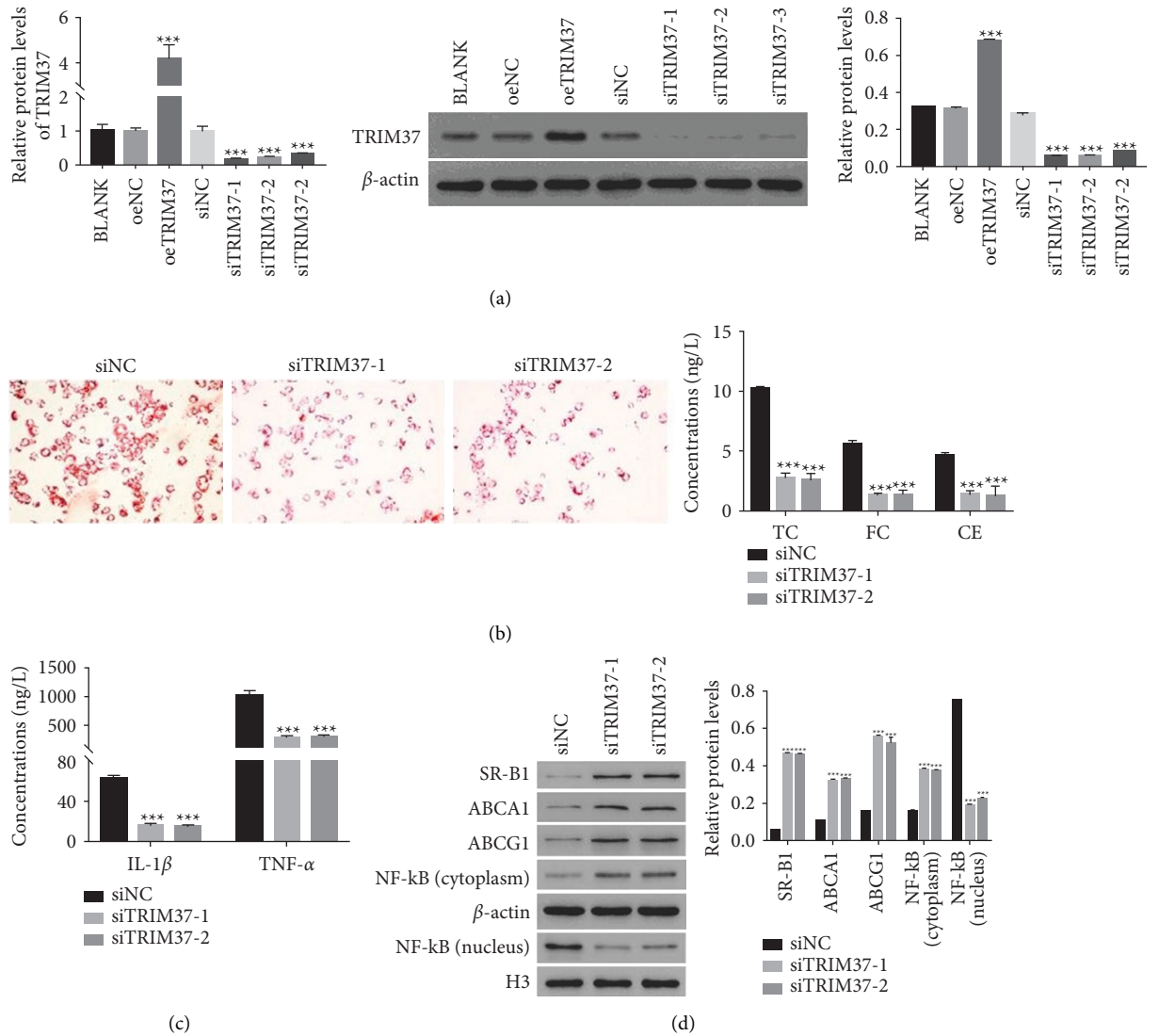


FIGURE 3: Overexpression and knockdown of TRIM37 and its silencing promoted cholesterol efflux in foam cells. (a) The relative mRNA levels and relative protein contents of TRIM37 in different transfected cells as indicated. \*\*\*  $P < 0.001$  vs. oeNC. (b) TRIM37 silencing inhibiting the uptake of oxLDL in foam cells. Magnification: 200x. TC, FC, and CE contents downregulated in siTRIM37-1 or siTRIM37-2 transfected cells. \*\*\*  $P < 0.001$  vs. siNC. (c) Knockdown of TRIM37 inhibiting the secretion of IL-1β and TNF-α in foam cells. \*\*\*  $P < 0.001$  vs. siNC. (d) Western blot used to quantify the protein content of SR-B1, ABCA1, ABCG1, NF-κB (cytoplasm), and NF-κB (nucleus) in cells as indicated above. \*\*\*  $P < 0.001$  vs. siNC.

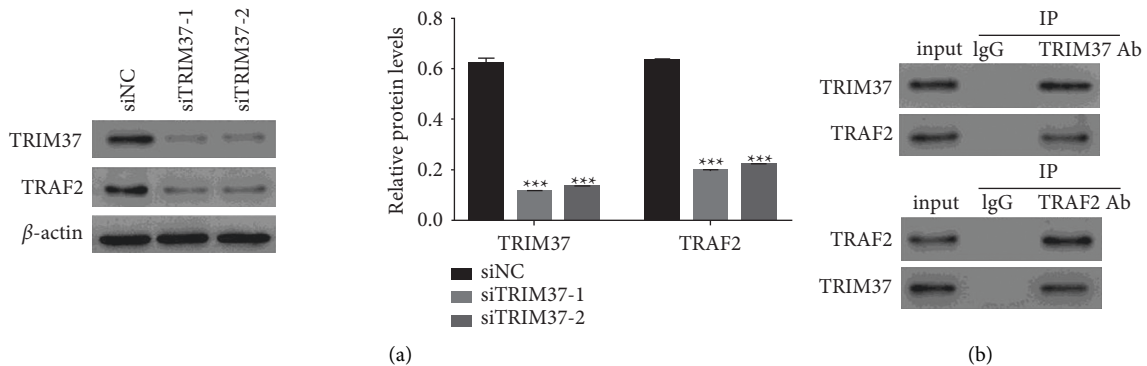


FIGURE 4: Continued.



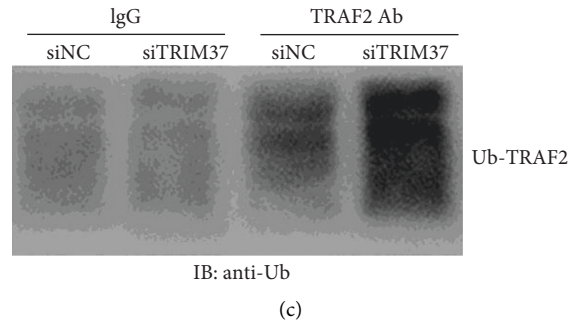


FIGURE 4: TRIM37 interacted with TRAF2 and negatively mediated its ubiquitination in foam cells. (a) The protein content of TRAF2 suppressed in siTRIM37-transfected cells.  $***P < 0.001$  vs. siNC. (b) TRIM37 interacting with TRAF2 in foam cells. (c) Knockdown of TRIM37 enhancing the ubiquitination of TRAF2 in foam cells.

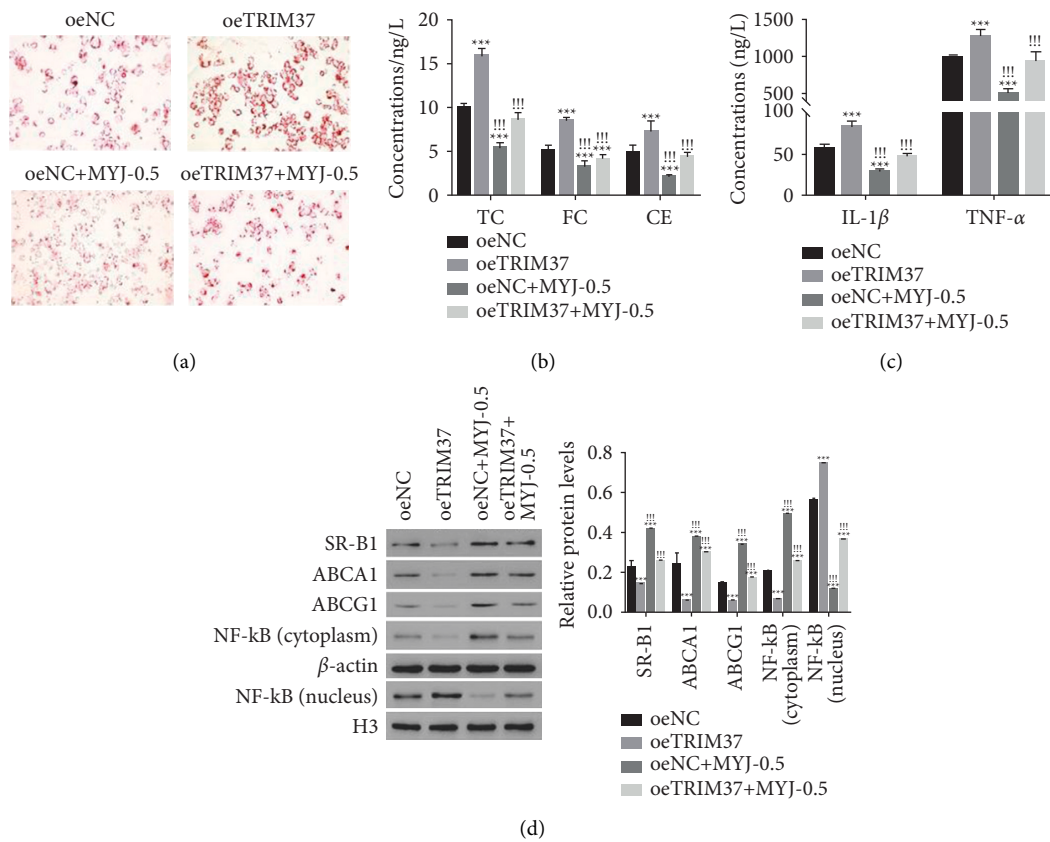


FIGURE 5: MYJ functioned as a TRIM37 inhibitor in foam cells. (a) MYJ treatment inhibiting the uptake of oxLDL in oeTRIM37-transfected cells. Magnification: 200x. (b) The accumulations of TC, FC, and CE downregulated in oeTRIM37-transfected cells in the presence of MYJ.  $***P < 0.001$  vs. oeNC;  $!!!p < 0.001$  vs. oeTRIM37. (c) The secretion of IL-1 $\beta$  and TNF- $\alpha$  inhibited in oeTRIM37-transfected cells with the treatment of MYJ.  $***P < 0.001$  vs. oeNC;  $!!!p < 0.001$  vs. oeTRIM37. (d) Western blot used to examine the contents of SR-B1, ABCA1, ABCG1, NF- $\kappa$ B (cytoplasm), and NF- $\kappa$ B (nucleus) in cells as indicated above.  $***P < 0.001$  vs. oeNC;  $!!!p < 0.001$  vs. oeTRIM37.

### 5. Conclusions

In this study, we investigated the function of MYJ in THP-1 macrophage-derived foam cells and explored its potential signaling pathway. Our findings demonstrated that MYJ was a promising agent in the treatment of atheroma and indicated its potential signaling pathway in foam cells.

### Abbreviations

- MYJ: Modified Yuejuwan
- oxLDL: Oxidatively modified low-density lipoprotein
- IL: Interleukin
- TNF: Tumor necrosis factor
- ELISA: Enzyme-linked immunosorbent assay

qRT-PCR: Quantitative PCR  
 TRIM37: Tripartite motif-containing 37  
 CVDs: Cardiovascular diseases  
 TRAF: TNF-receptor associated factor  
 NF- $\kappa$ B: Nuclear factor- $\kappa$ B  
 TCM: Traditional Chinese medicine  
 PBS: Phosphate buffer solution  
 siRNA: Short interfering RNAs  
 oeNC: Corresponding negative control  
 FC: Free cholesterol  
 T-CHO: Total cholesterol  
 CE: Cholesteryl ester  
 Co-IP: Coimmunoprecipitation  
 RIPA: Radioimmunoprecipitation assay.

### Data Availability

The datasets used and/or analyzed during the current study are available from the corresponding author upon request.

### Consent

Not applicable.

### Disclosure

The sponsor had no role in the design or analysis of this study or the interpretation of the findings.

### Conflicts of Interest

The authors declare that they have no conflicts of interest.

### Authors' Contributions

Deyu Fu designed this project and wrote the manuscript. MingtaiGui performed the experiments. Lei Yao, Bo Lu, and Jianhua Li analyzed the data and edited diagrams. Jing Wang and Xunjie Zhou helped to collect data. All authors have contributed to read and agreed to the final content of the manuscript for submission.

### Acknowledgments

The authors acknowledged the assistance given by the Yueyang Hospital of Integrated Traditional Chinese and Western Medicine, Shanghai University of Traditional Chinese Medicine Shanghai, P.R. China. This work was supported by the National Nature Science Foundation of China (81774111), Shanghai Municipal Planning Commission of Science and Research Fund (20184Y0285), and Shanghai Three-Year Project of Traditional Chinese Medicine (2018-2020): cardiology of traditional Chinese medicine.

### References

- [1] Y. T. Lee, H. Y. Lin, Y. W. F. Chan et al., "Mouse models of atherosclerosis: a historical perspective and recent advances," *Lipids in Health and Disease*, vol. 16, no. 1, p. 12, 2017.
- [2] N. Previsani, D. Lavanchy, and World Health Organization, "Fact sheet," *Indian Journal of Chest Diseases & Allied Sciences*, vol. 42, no. 2, pp. 126–128, 2000.
- [3] G. S. Getz and C. A. Reardon, "Animal models of atherosclerosis," *Arteriosclerosis, Thrombosis, and Vascular Biology*, vol. 32, no. 5, pp. 1104–1115, 2012.
- [4] X.-H. Yu, K. Qian, N. Jiang, X.-L. Zheng, F. S. Cayabyab, and C.-K. Tang, "ABCG5/ABCG8 in cholesterol excretion and atherosclerosis," *Clinica Chimica Acta*, vol. 428, pp. 82–88, 2014.
- [5] J. H. Qiao, J. Tripathi, N. K. Mishra et al., "Role of macrophage colony-stimulating factor in atherosclerosis: studies of osteopetrotic mice," *American Journal of Pathology*, vol. 150, no. 5, pp. 1687–1699, 1997.
- [6] E. M. Maguire, S. W. A. Pearce, and Q. Xiao, "Foam cell formation: a new target for fighting atherosclerosis and cardiovascular disease," *Vascular Pharmacology*, vol. 112, pp. 54–71, 2019.
- [7] J. Kallijärvi, U. Lahtinen, R. Hämäläinen, M. Lipsanen-Nyman, J. J. Palvimö, and A. E. Lehesjoki, "TRIM37 defective in mulibrey nanism is a novel RING finger ubiquitin E3 ligase," *Experimental Cell Research*, vol. 308, no. 1, pp. 146–155, 2005.
- [8] S. K. Goru, A. Pandey, and A. B. Gaikwad, "E3 ubiquitin ligases as novel targets for inflammatory diseases," *Pharmacological Research*, vol. 106, pp. 1–9, 2016.
- [9] Y. Li, L. Deng, X. Zhao et al., "Tripartite motif-containing 37 (TRIM37) promotes the aggressiveness of non-small-cell lung cancer cells by activating the NF- $\kappa$ B pathway," *The Journal of Pathology*, vol. 246, no. 3, pp. 366–378, 2018.
- [10] S. Brauner, X. Jiang, G. E. Thorlacius et al., "Augmented Th17 differentiation in Trim21 deficiency promotes a stable phenotype of atherosclerotic plaques with high collagen content," *Cardiovascular Research*, vol. 114, no. 1, pp. 158–167, 2018.
- [11] T. Yoshida, M. Yamashita, C. Horimai, and M. Hayashi, "Smooth muscle-selective inhibition of nuclear factor- $\kappa$ B attenuates smooth muscle phenotypic switching and neointima formation following vascular injury," *Journal of American Heart Association*, vol. 2, no. 3, Article ID e000230, 2013.
- [12] Y. Wang, X. Wang, M. Sun, Z. Zhang, H. Cao, and X. Chen, "NF- $\kappa$ B activity-dependent P-selectin involved in ox-LDL-induced foam cell formation in U937 cell," *Biochemical and Biophysical Research Communications*, vol. 411, no. 3, pp. 543–548, 2011.
- [13] Y. Si, Y. Zhang, J. Zhao et al., "Niacin inhibits vascular inflammation via downregulating nuclear transcription factor- $\kappa$ B signaling pathway," *Mediators of Inflammation*, vol. 2014, Article ID 263786, 12 pages, 2014.
- [14] J. D. Plotkin, M. G. Elias, A. L. Dellinger, and C. L. Kopley, "NF- $\kappa$ B inhibitors that prevent foam cell formation and atherosclerotic plaque accumulation," *Nanomedicine: Nanotechnology, Biology and Medicine*, vol. 13, no. 6, pp. 2037–2048, 2017.
- [15] L. Ren and G. Chen, "Rapid antidepressant effects of Yueju: a new look at the function and mechanism of an old herbal medicine," *Journal of Ethnopharmacology*, vol. 203, pp. 226–232, 2017.
- [16] Z. M. Hao, Y. S. Zhao, W. P. Zhu, and X. C. Jin, "Effect of modified YueJuWan on adiponectin and leptin in the serum of nonalcoholic fatty liver disease rat," *Progress in Modern Biomedicine*, vol. 13, no. 18, pp. 3428–3431, 2013.
- [17] Y. Xu, "Study on treating 60 NAFLD cases through phlegm and blood stasis dispelling," *Liaoning Journal of Traditional Chinese Medicine*, vol. 28, no. 10, pp. 612–613, 2001.



- [18] T. Fu, "Clinical observation of treating 48 NAFLD cases by means of activating spleen, removing phlegm and dissolving food retention," *Henan Traditional Chinese Medicine*, vol. 28, no. 9, pp. 55-56, 2008.
- [19] M. Daigneault, J. A. Preston, H. M. Marriott, M. K. B. Whyte, and D. H. Dockrell, "The identification of markers of macrophage differentiation in PMA-stimulated THP-1 cells and monocyte-derived macrophages," *PLoS One*, vol. 5, no. 1, Article ID e8668, 2010.
- [20] N. Wang, J.-Y. Li, S. Li et al., "Fibroblast growth factor 21 regulates foam cells formation and inflammatory response in Ox-LDL-induced THP-1 macrophages," *Biomedicine & Pharmacotherapy*, vol. 108, pp. 1825-1834, 2018.
- [21] H. Wang, Y. Li, X. Zhang, Z. Xu, J. Zhou, and W. Shang, "DPP-4 inhibitor linagliptin ameliorates oxidized LDL-induced THP-1 macrophage foam cell formation and inflammation," *Drug Design, Development and Therapy*, vol. 14, pp. 3929-3940, 2020.
- [22] H. Tilg and A. M. Diehl, "Cytokines in alcoholic and non-alcoholic steatohepatitis," *New England Journal of Medicine*, vol. 343, no. 20, pp. 1467-1476, 2000.
- [23] R. Out, M. Hoekstra, K. Habets et al., "Combined deletion of macrophage ABCA1 and ABCG1 leads to massive lipid accumulation in tissue macrophages and distinct atherosclerosis at relatively low plasma cholesterol levels," *Arteriosclerosis, Thrombosis, and Vascular Biology*, vol. 28, no. 2, pp. 258-264, 2008.
- [24] D. D. Feng, T. Tang, X. P. Lin et al., "Nine traditional Chinese herbal formulas for the treatment of depression: an ethnopharmacology, phytochemistry, and pharmacology review," *Neuropsychiatric Disease and Treatment*, vol. 12, pp. 2387-2402, 2016.
- [25] G. E. Ke-Min, W. Wang, W. D. Xue, G. Chen, and F. S. Wang, "Neuroprotective effect of modified yuejuwan and ganmai dazao tang on glutamate-induced HT22 cell injury model," *Chinese Journal of Experimental Traditional Medical Formulae*, vol. 24, pp. 22-27, 2019.
- [26] W. Zhang, S. H. Tang, Y. Zhang et al., "[Study on Yueju Wan for 'different diseases with same treatment' based on integrative pharmacology]," *Zhongguo Zhong Yao Za Zhi*, vol. 43, no. 7, pp. 1352-1359, 2018.
- [27] G. J. Randolph, "Mechanisms that regulate macrophage burden in atherosclerosis," *Circulation Research*, vol. 114, no. 11, pp. 1757-1771, 2014.
- [28] Z. G. Huang, C. Liang, S. F. Han, and Z. G. Wu, "Vitamin E ameliorates ox-LDL-induced foam cells formation through modulating the activities of oxidative stress-induced NF- $\kappa$ B pathway," *Molecular and Cellular Biochemistry*, vol. 363, no. 1-2, pp. 11-19, 2012.
- [29] H. Tian, S.-T. Yao, N.-N. Yang et al., "D4F alleviates macrophage-derived foam cell apoptosis by inhibiting the NF- $\kappa$ B-dependent Fas/FasL pathway," *Scientific Reports*, vol. 7, no. 1, p. 7333, 2017.
- [30] B. Brigant, V. Metzinger-Le Meuth, J. Rochette, and L. Metzinger, "TRIMming down to TRIM37: relevance to inflammation, cardiovascular disorders, and cancer in MULLIBREY nanism," *International Journal of Molecular Sciences*, vol. 20, no. 1, 2018.
- [31] F. Meitinger, M. Ohta, K.-Y. Lee et al., "TRIM37 controls cancer-specific vulnerability to PLK4 inhibition," *Nature*, vol. 585, no. 7825, pp. 440-446, 2020.
- [32] X.-H. Yu, X.-L. Zheng, and C.-K. Tang, "Nuclear factor- $\kappa$ B activation as a pathological mechanism of lipid metabolism and atherosclerosis," *Advances in Clinical Chemistry*, vol. 70, pp. 1-30, 2015.
- [33] J. L. Pomerantz and D. Baltimore, "NF-kappa B activation by a signaling complex containing TRAF2, TANK and TBK1, a novel IKK-related kinase," *The EMBO Journal*, vol. 18, no. 23, pp. 6694-6704, 1999.
- [34] W. Wang, Z.-J. Xia, J.-C. Farré, and S. Subramani, "TRIM37, a novel E3 ligase for PEX5-mediated peroxisomal matrix protein import," *Journal of Cell Biology*, vol. 216, no. 9, pp. 2843-2858, 2017.